RSC Advances

PAPER

Check for updates

Cite this: *RSC Adv.*, 2023, **13**, 18138

Nanoscale carbon dot-embedded metal–organic framework for turn-on fluorescence detection of water in organic solvents†‡

Theanchai Wiwasuku,[ad] Jitti Suebphanpho,[a] Somlak Ittisanronnachai,[b] Vinich Promarak,[c] Jaursup Boonmak*[a] and Sujittra Youngme[a]

An easy-to-use, highly selective, and real-time organic solvent quality assessment is desirable to detect water contamination in organic solvents. Herein, a one-step procedure using ultrasound irradiation was used for encapsulating nanoscale carbon dots (CDs) into metal–organic framework-199 (HKUST-1) to form CDs@HKUST-1 composite. The CDs@HKUST-1 exhibited very weak fluorescence due to photo-induced electron transfer (PET) from the CDs to the Cu^{2+} centers, acting as a fluorescent sensor in its off-state. The designed material can detect and discriminate water from other organic solvents, driven by turn-on fluorescence. This highly sensitive sensing platform could be applied for the detection of water in ethanol, acetonitrile, and acetone with wide linear detection ranges of 0–70% v/v, 2–12% v/v, and 10–50% v/v and limits of detection of 0.70% v/v, 0.59% v/v, and 1.08% v/v, respectively. The detection mechanism is attributed to the interruption of the PET process due to the release of fluorescent CDs after treatment with water. A smartphone-based quantitative test was successfully developed to monitor the water content in organic solvents utilizing CDs@HKUST-1 and a phone color processing application, thus making it possible to develop an on-site, real time and easy-to-use sensor for water detection.

Received 10th January 2023
Accepted 15th May 2023

DOI: 10.1039/d3ra00195d

rsc.li/rsc-advances

1 Introduction

Organic solvents contaminated with water not only impacts the stability and physicochemical qualities of chemicals and medicines, but also affects their efficacy and usage.[1,2] The water content of reaction materials and solvents also has a significant impact on the yield and selectivity of many sensitive chemical processes.[3] Various traditional techniques including Karl Fischer titration,[4] chromatography,[5] electrochemical analysis[6] and spectroscopic approaches,[7–9] have been used to monitor water content in organic solvents. However, these techniques normally require specialized equipment and expert operators, are high cost and time-consuming. Therefore, the development of a simple, quick, and reliable method for water assessment in organic solvents is essential for chemical synthesis and manufacturing industries. Recently, fluorescence methods have been considered one of the most efficient approaches for chemical detection owing to their ease of use, cost-effectiveness, fast response, and visual detection potential.[10,11] Metal–organic frameworks (MOFs), a type of crystalline material in which metal ions/clusters serve as nodes and organic ligands act as struts, have attracted more and more attention as fluorescent sensory materials because of their large specific surface areas, adjustable pore sizes, and tuneable sensing performance.[12,13] In particular, MOFs can sense targets through unique interactions between the organic ligand and/or metal units of MOFs and a target, contributing to the fast response, high selectivity, and sensitivity of MOF-based fluorescent probes.[14–16] Several MOFs have been utilized as fluorescent probes for water sensing in organic solvents.[3,17–23] These MOFs are mostly derived from rare earth metals (Tb^{3+} and Eu^{3+}) and transition metals (Cd^{2+} and Zn^{2+}). However, lanthanide metals are expensive and scarce, and certain metal ions, for example Cd^{2+}, are very hazardous. Additionally, the detection of water using these reported MOFs is constrained as follows: (i) the procedure is difficult and requires the heating of MOFs to generate dehydrated MOFs; (ii) they exhibit a narrow detection range; (iii) water sensors based on MOFs normally work *via* luminescence turn-off, whereas the

[a]*Materials Chemistry Research Center and Center of Excellence for Innovation in Chemistry, Department of Chemistry, Faculty of Science, Khon Kaen University, Khon Kaen, 40002, Thailand. E-mail: jaursup@kku.ac.th*

[b]*Frontier Research Center (FRC), Vidyasirimedhi Institute of Science and Technology, Rayong, 21210, Thailand*

[c]*Department of Materials Science and Engineering, School of Molecular Science and Engineering, Vidyasirimedhi Institute of Science and Technology, Rayong, 21210, Thailand*

[d]*Functional Materials and Nanotechnology Center of Excellence, School of Science, Walailak University, Nakhon Si Thammarat, 80160, Thailand*

† This work is dedicated to Professor Sujittra Youngme, Khon Kaen University, Thailand, on the occasion of her retirement.

‡ Electronic supplementary information (ESI) available. See DOI: https://doi.org/10.1039/d3ra00195d

This article is licensed under a Creative Commons Attribution-NonCommercial 3.0 Unported Licence.

© 2023 The Author(s). Published by the Royal Society of Chemistry

turn-on process has been rarely reported. Compared with turn-off sensing, the turn-on signal is more easily visible to the naked eye, which is more sensitive and simpler for in-field detection.[24] In light of this, the development and exploration of an effective, environmentally friendly, low-cost, and easy-to-use water sensor is challenging but necessary.

Carbon dot-embedded MOFs (CDs@MOF) are promising candidates for water sensing in organic solvents. This is due to the low toxicity of CDs, ease of synthesis, high water solubility, high quantum yield, and ease of functionalization.[25,26] CDs@MOF composites incorporate the benefits of both CDs and MOFs, including: the outstanding optical characteristics of CDs such as adjustable emission lights, high quantum yields, and photochemical durability;[27,28] as well as the tunable pore size and shape, high surface area, and abundant active sites of MOFs,[29,30] resulting in increased sensing performance. MOFs encapsulating carbon dots have been reported as fluorescent sensors for detecting water molecules in organic solvents. To the best of our knowledge, CDs@MOF-based fluorescent water sensors based on the inhibition of the photo-induced electron transfer (PET) process, have not been reported to date. The PET phenomenon has recently been exploited to develop turn-on sensors.[31] In PET-based sensors, excited electrons are transferred from the excited fluorophore to the quenching agent, resulting in a reduction in fluorescence luminosity. The natural fluorescence of the fluorophore can be recovered following host–guest interaction between target molecules and the sensory probe, causing the PET process to be interrupted.

In the present work, a CDs@HKUST-1 composite was prepared using a simple and environmentally friendly method by encapsulating CDs into a copper-based MOF (MOF-199 defined as HKUST-1), using an ultrasound-assisted method. Nanoscale CDs were loaded into HKUST-1 to function as blue emission centers of CDs@HKUST-1 and to boost sensing sensitivity. Because of its large pore diameter and functional pore surface, HKUST-1 is not only a host framework for loading CDs, but it can also trap guest molecules. This leads to the pre-concentration of the analytes, providing good performance for the detection (Fig. 1). The prepared CDs@HKUST-1 presented very weak emission, which resulted from PET from CDs to Cu^{2+} centers in HKUST-1. Interestingly, the strong bright fluorescence of CDs@HKUST-1 was significantly recovered after the addition of water to other organic solvents. The proposed CDs@HKUST-1 demonstrated the selective detection of trace water based on a fluorescence turn-on assay with wide linear detection ranges of 0–70% v/v, 2–12% v/v, and 10–50% v/v and limits of detection (LODs) of 0.70% v/v, 0.59% v/v, and 1.08% v/v for the sensing in ethanol, acetronitrile, and acetone, respectively. Using a mobile phone application for the analysis of the RGB value, CDs@HKUST-1 and a smartphone were successfully integrated to monitor the water content in organic solvents.

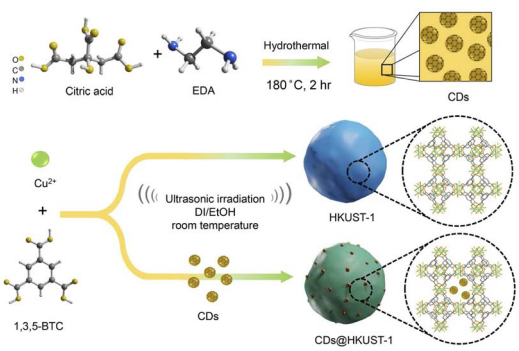

Fig. 1 Schematic illustration of the preparation of CDs and ultrasonic-assisted synthesis of HKUST-1 and CDs@HKUST-1 reaction pathways at room temperature.

2 Experimental methods

2.1 Materials and physical measurements

All reagents were obtained from commercial sources and used as received without further purification. The FT-IR spectra were recorded in the frequency range 4000–600 cm^{-1} on a Bruker Tensor 27 FT-IR spectrophotometer with a standard Pike ATR cell. A Shimadzu UV 2450 spectrometer was used to record the UV-vis spectra in solution. Powder X-ray diffraction (PXRD) experiments were conducted on a Bruker D8 ADVANCE diffractometer with Cu Kα radiation at the 2θ range of 5–50°. Photoluminescence spectra were obtained using a Shimadzu RF-6000 spectrofluorometer at room temperature. Transmission electron microscopy (TEM) was undertaken using an FEI Tecnai G2 S-Twin transmission electron microscope. Scanning electron microscopy (FESEM) was done using a JEOL JSM-7500F field emission scanning electron microscope. Energy dispersive X-ray spectroscopy (EDS) was done using a Merlin Compact scanning electron microscope. The metal content analysis was performed on an atomic absorption spectrometer (AAS) using PerkinElmer PinAAcle 900F. X-ray photoelectron spectroscopy (XPS) was recorded using a JEOL JPS-9010MC with a twin anode (Mg Kα source, 1253.6 eV and Al Kα source, 1486.6 eV) at 12 kV and 25 mA. Gas adsorption–desorption was measured using a MicrotracBEL/BELSORP-mini II at the desired temperature.

2.2 Synthesis of CDs

CDs were simply prepared according to the reported method with some modifications.[32] Briefly, 1.025 g of citric acid was completely dissolved in 10 mL of DI water. Then, 335 mL of ethylenediamine (EDA) was immediately added. The mixture was transferred to a 25 mL Teflon lined hydrothermal autoclave and heated at 180 °C for 2 h. A brown solution was eventually obtained after cooling to room temperature, and filtered using a membrane, and then stored in the dark for later use.

2.3 Synthesis of CDs@HKUST-1 and HKUST-1

The nanoscale CDs@HKUST-1 was prepared using an ultrasonic-assisted environmentally friendly method. In brief, 2 mL of CDs was added to 0.0525 g of benzene-1,3,5-tricarboxylic acid in 2 mL of DI water and 6 mL of ethanol. The mixed solution was then placed into an ultrasonic bath. $Cu(CH_3COO)_2 \cdot nH_2O$ (0.0.0815 g) in DI water was slowly added

© 2023 The Author(s). Published by the Royal Society of Chemistry

to the mixture, and a green precipitate suddenly formed under ultrasonic irradiation with a maximum power output of 280 W and a frequency of 50/60 Hz. The reaction time was 30 min. The CDs@HKUST-1 composite was obtained by centrifugation at 6000 rpm for 10 min, washed five times with 10 mL of methanol, and dried at 50 °C. The dried product was then ground to obtain the CDs@HKUST-1 composite powder, which was then kept in the dark for later use.

HKUST-1 was synthesized *via* a sonochemical method using a similar procedure to CDs@HKUST-1, except that CDs were not added.

2.4 Fluorescence detection of water in organic solvents (EtOH, acetone, and ACN)

For the sensing experiment, 10 mg of finely ground CDs@HKUST-1 was dispersed in 20 mL of dried ethanol and sonicated for 5 minutes to form a suspension. 500 μL of the CDs@HKUST-1 suspension was added to 4 mL of the ethanol–water solution containing a known water content (0–70% v/v). After 45 min of incubation, the luminescence spectra were measured with an excitation wavelength of 365 nm. The processes for the detection of water in dried acetone and ACN are similar to that for the detection of water in ethanol, except that dried acetone and dried ACN were used instead of dried ethanol.

3 Results and discussion

3.1 Characterization of CDs@HKUST-1

The encapsulation of CDs into HKUST-1 to fabricate the CDs@HKUST-1 composite were rapidly produced by the ultrasound-assisted method, which is environmentally friendly, simple, inexpensive, and high throughput. The CDs@HKUST-1 powder was obtained in green compared with the pristine HKUST-1 which is bright blue (Fig. S1(a and b)‡), so the colour change indicated that CDs were successfully embedded in the MOF. The Tyndall effect, which occurs when highly distributed CDs@HKUST-1 composite in ethanol scatters an incoming laser light beam, was verified to exist in such a colloidal ethanol suspension of CDs@HKUST-1, as presented in Fig. S1(c and d).‡

Transmission electron microscopy (TEM) and scanning electron microscopy (SEM) were used to investigate the morphology of the obtained CDs and CDs@HKUST-1. As shown in Fig. 2(a), the prepared nanoscale CDs are spherical with a size distribution of 3.48 ± 0.63 nm (Fig. S2‡). As can be seen in Fig. 2(b and c), the morphology of composite CDs@HKUST-1 particles are consistent with those of pristine HKUST-1. Fig. 2(d) shows the incorporation of CDs into HKUST-1, indicating the successful formation of the CDs@HKUST-1 composite. SEM images of HKUST-1 and CDs@HKUST are shown in Fig. 2(e and f). It is evident that HKUST-1 and CDs@HKUST-1 have almost octahedral nanoparticles with diameters of about 97.55 ± 25.63 nm and 145.66 ± 33.11 nm, respectively. As seen in the SEM images, the morphology of HKUST-1 is not significantly affected by the incorporation of CDs. SEM element mapping revealed that C, N, O, and Cu

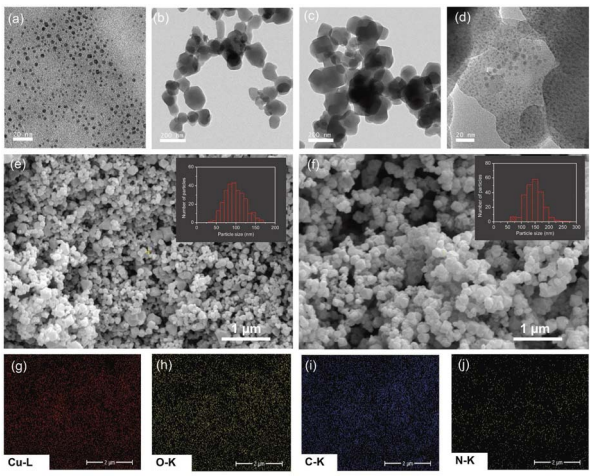

Fig. 2 TEM images of (a) CDs, (b) HKUST-1, and (c and d) CDs@HKUST particles. SEM images of (e) HKUST-1 and (f) CDs@HKUST-1. The inset of (e) and (f) show the size distribution histograms. The corresponding element mapping images of (g) Cu, (h) O, (i) C, and (j) N of CDs@HKUST-1 composite.

elements were uniformly distributed in CDs@HKUST-1 (Fig. 2(g–j)).

The PXRD pattern of the as-synthesized HKUST-1 and CDs@HKUST-1 matched the as-simulated pattern (Fig. 3(a)). This suggests that CDs@HKUST-1 could be synthesized and the CDs have no effect on the fundamental framework structure. The FT-IR spectra of HKUST-1 and CDs@HKUST-1 were also characterized. Compared with the FT-IR spectra of HKUST-1, the additional stretching vibration peaks C–H in the methyl group (2983 and 2900 cm^{-1}), C═O in the carboxyl group (1740 cm^{-1}), C–O (1076 cm^{-1}), and C–N (1024 cm^{-1}) of the CDs were observed in CDs@HKUST-1 (Fig. 3(b)).[33,34] This shows that CDs were effectively embedded into HKUST-1. N_2 adsorption–desorption isotherms were performed on the HKUST-1 and CDs@HKUST-1 composite materials. Fig. S3‡ illustrates the N_2 adsorption–desorption isotherms of the samples. From the adsorption isotherms (Fig. S3(a)‡), the Brunauer–Emmett–Teller (BET) surface areas of 1144.8 $m^2\ g^{-1}$, a pore volume of 1.0677 $cm^3\ g^{-1}$, and average pore diameter of 3.7307 nm were found for HKUST-1 (Table S1‡). CDs@HKUST-1 exhibits a similar isotherm profile with a decrease in the adsorbed N_2 volume (Fig. S3(b)‡). The BET surface areas of CDs@HKUST-1 slightly increased (Table S1‡). Significantly, the pore volume and pore diameter of CDs@HKUST-1 were smaller than for HKUST-1, indicating that some of the MOF pores were occupied or blocked by the CDs.

According to the XPS analysis of HKUST-1 before and after the addition of CDs (Fig. 3(c)), the Cu 2p, O 1s, and C 1s of HKUST-1 and the N 1s of CDs (inset of Fig. 3(c)) could be detected in the CDs@HKUST-1 survey spectrum. The high-resolution Cu 3p peaks of CDs@HKUST-1 were negatively shifted to a lower binding energy than those of HKUST-1, as shown in Fig. S4(a).‡ This is due to the interaction between the carboxyl functional group on CDs and the Cu(II) center in the MOF. In Fig. S4(b),‡ the high-resolution C 1s spectra revealed that it

© 2023 The Author(s). Published by the Royal Society of Chemistry

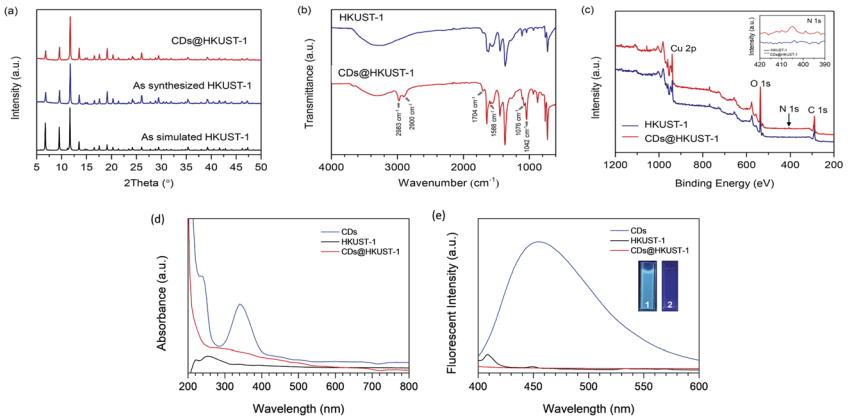

Fig. 3 (a) PXRD patterns of the as-simulated HKUST-1, as-synthesized HKUST-1, and CDs@HKUST-1. (b) FT-IR spectra of HKUST-1 and CDs@HKUST-1. (c) Wide scan XPS spectra of HKUST-1 and CDs@HKUST-1. The inset shows the magnified XPS spectra in the region 390–420 eV. (d) UV-vis absorption spectra of CDs, HKUST-1, and CDs@HKUST-1. (e) Fluorescence spectra of CDs, HKUST-1, and CDs@HKUST-1 with excitation wavelength 365 nm. The inset exhibits the photographs of (1) CDs and (2) CDs@HKUST-1 in ethanol under UV-light (365 nm).

could also be deconvoluted into four peaks at 284.26, 284.88, 285.49, and 288.53 eV, which were attributed to the C=C, C–C, C=O, and N–C=O, respectively. The distinctive Cu–O and O–C=O peaks at 531.82 and 533.47 eV, respectively, were observed in the high-resolution O 1s spectra in Fig. S4(c).‡ A small amount of N was detected in CDs@HKUST-1 according to the high resolution N 1s spectra (inset of Fig. 3(c)), two peaks at 399.15 and 400.40 eV were identified as C–N and $-NH_2$, respectively (Fig. S4(d)‡). The aforementioned results further proved that CDs were effectively encapsulated in CDs@HKUST-1.

The UV-visible absorption and fluorescence spectra of CDs, HKUST-1 and CDs@HKUST-1 were investigated and are displayed in Fig. 3(d and e). From Fig. 3(d), we can see the prepared CDs present with an absorption peak at around 225 nm, regarded as the π–π* transition of C=C bonds, while the broad absorption peak at 345 nm may be attributed to the n–π* transition of C=O on the surface of the CDs. HKUST-1 exhibits a distinct absorption peak below 300 nm, while CDs@HKUST-1 showed absorption at 300–550 nm, which corresponds to the CDs' distinctive absorption band, suggesting the incorporation of CDs into the HKUST-1 structure. As depicted in Fig. 3(e), with excitation at 365 nm, HKUST-1 showed no distinct fluorescence emission. In contrast, the CDs dispersed in ethanol displayed a strong blue fluorescence at 450 nm. When CDs were introduced in to HKUST-1, the fluorescence intensity of CDs in the CDs@HKUST-1 composite was significantly diminished. Under UV light irradiation, CDs@HKUST-1 is almost non-emissive when compared with pure CDs (inset of Fig. 3(e)). This is attributed to the binding interaction between the carboxyl group on the surface of CDs and the Cu^{2+} of HKUST-1, resulting in electron transfer from CDs to Cu^{2+} with reduced electron density on CDs. As a result, the surface state of CDs was altered, enabling effective fluorescence quenching of CDs in CDs@HKUST-1.[22] Based on the very weak fluorescence of CDs@HKUST-1, it could be used as a fluorescent probe in a turn-on strategy.

3.2 Fluorescence sensing of water in organic solvents

To explore the fluorescence sensing of water, we carried out fluorescence measurements of CDs@HKUST-1 in water and pure dried organic solvents including dimethylformamide (DMF), methanol (MeOH), ethanol (EtOH), acetonitrile (ACN), iso-propanol (iso-PrOH), acetone, dichloromethane (DCM), ethyl acetate (EtOAc), tetrahydrofuran (THF), toluene, hexane, and 1,4-dioxane. Interestingly, the proposed CDs@HKUST-1 sensor shows the highest fluorescence intensity in water when compared with the other solvents, as shown in Fig. 4(a and b). This indicates that CDs@HKUST-1 has excellent selectivity for water and can discriminate water from other organic solvents. Furthermore, a fluorescence titration experiment using CDs@HKUST-1 in EtOH with the addition of different water volumes was performed. As presented in Fig. 4(c), the

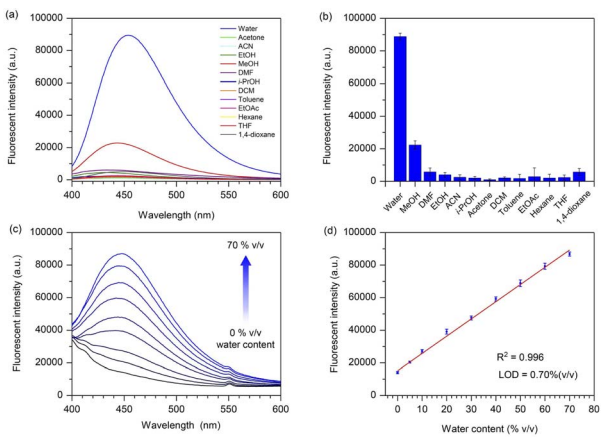

Fig. 4 (a) Fluorescence spectra and (b) fluorescence intensity at 450 nm (λ_{ex} = 365 nm) for CDs@HKUST-1 in various solvents, (c) the fluorescence spectra of CDs@HKUST-1 in EtOH solution with the incremental addition of water content from 0–70% v/v. (d) The linear relationship between the fluorescence intensity at 450 nm and water content (0–70% v/v).

© 2023 The Author(s). Published by the Royal Society of Chemistry

fluorescence of CDs@HKUST-1 was dramatically increased with increasing water content. The linear regression equation of the fluorescence intensity at 450 nm and water content change from 0% to 70% v/v can be written as $y = 1053.335x + 15\,306.820$ and the R^2 value is 0.996, indicating the detection range of water in ethanol is in the range 0–70% v/v. In accordance with the formula LOD = $3\sigma/S$ (σ = a standard deviation of the fluorescence test for 7 blank solutions, S is the slope of the linear equation),[3] the limit of detection (LOD) of CDs@HKUST-1 for water in ethanol was calculated to be as low as 0.70% v/v as shown in Table S2.‡ The obtained LOD is less than that found in AEHC (hydrated ethyl alcohol fuel; 0.8% in China, 1.0% in the US, and 4.9% in Brazil).[35] The fluorescence response of CDs@HKUST-1 toward water was also examined in ACN and acetone under the same conditions as in EtOH, the results are displayed in Fig. S5.‡ It was revealed that the fluorescence of CDs@HKUST-1 in ACN and acetone, was gradually raised with increasing water content. A good linear relationship between fluorescence intensity and water content was obtained in the range 2–12% v/v and 10–50% v/v for ACN and acetone, respectively. The LODs of water in ACN and acetone were calculated to be 0.59 and 1.08% v/v, respectively. This finding demonstrates the ability of CDs@HKUST-1 to detect water content in EtOH, ACN, and acetone. As shown in Table S3,‡ the observed LODs for water in organic solvents using the CDs@HKUST-1 composite are significantly higher than other reported MOFs. CDs@HKUST-1, on the other hand, had a wider detection range, making this material more practical to use. Moreover, it is still very cost-effective and environmentally friendly in comparison to lanthanide-based MOFs, lanthanide-doped MOFs, and cadmium-based MOFs. This exemplifies the outstanding environmental and economic possibilities of using CDs@HKUST-1 as an effective sensor for water in organic solvents.

In addition, the reaction time on the fluorescence intensity of the materials was studied. As shown in Fig. S6(a),‡ the fluorescence was enhanced within 1 min of injecting 50% v/v water into an ethanol solution containing CDs@HKUST-1, suggesting that the material responds rapidly to water. The fluorescence signal remained unchanged thereafter. The anti-interference performance of CDs@HKUST-1 toward water in the presence of organic solvent was also determined. The fluorescence of the sensor was significantly increased after incorporating several solvents with 50% v/v water, as illustrated in Fig. S6(b),‡ suggesting the good anti-interference capability of the material. In light of these findings, the CDs@HKUST-1 composite is a fluorescence sensor with excellent sensitivity, selectivity, and good anti-interference capabilities for rapid detection of water.

3.3 Smartphone-based fluorometric sensing of water

To establish a quick, practical, and on-site detection method for water sensing in organic solvents, a smartphone application was used as a signal collector and analyzer to detect water in organic solvents. As shown in Fig. 5(a), the fluorescence of the reaction solution progressively changed from dark to bright blue with increasing water content under UV light (365 nm).

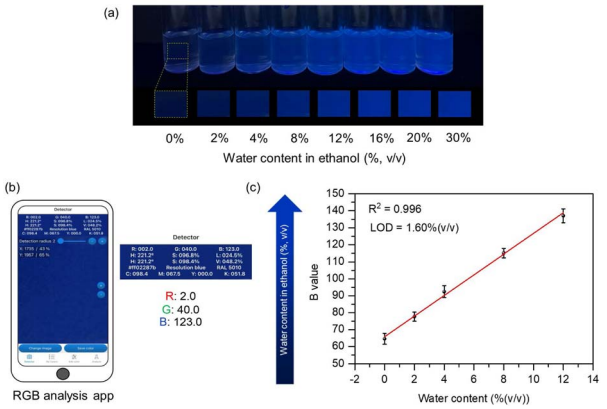

Fig. 5 (a) Digital images of fluorescence change of CDs@HKUST-1 with different water content in ethanol under UV light (365 nm). (b) Smartphone application of RGB analysis for quantitative detection of water in organic solvents. (c) Linear relationship between B value and water levels (0–12% v/v) in ethanol.

This turn-on fluorescence induced by water could be simply and visibly detected by the naked eye. The images of samples were taken using a smartphone camera, and the color of the images was converted into color information (red, green, and blue (RGB) value) by the ColorDetector (Fig. 5(b)). As seen in Fig. 5(c), a good linear relationship ($R^2 = 0.996$) between the B value and the water content in ethanol was obtained in the range 0–12% v/v with an LOD of 1.60% v/v. Therefore, on-site detection based on a smartphone integrated sensing platform for water in acetone and ACN can be developed. The results show good linear detection ranges from 0–16% v/v and 2–16% v/v with LODs of 2.44% v/v and 2.52% v/v in acetone and ACN, respectively (Fig. S7‡). Despite the higher detection limit observed for the fluorescence analysis based on CDs@HKUST-1 (Section 3.2), the use of the portable handheld device offers several benefits and illustrates that without the assistance of specialized equipment, a smartphone-assisted CDs@HKUST-1 sensor is clearly easier to use and more suited for practical applications.

3.4 Fluorescence enhancement mechanism

CDs@HKUST-1 exhibited fluorescent enhancement in the presence of water molecules. In contrast, the fluorescent signal of individual CDs did not significantly change in the presence of water (Fig. S8‡). This suggests that the infrastructure of HKUST-1 in the composite plays an important role in recognizing and responding to water molecules. As shown in Fig. S9(a and b),‡ the octahedral particles of CDs@HKUST-1 changed into large numbers of tiny irregular nanoparticles after treating with water, suggesting that water can affect the morphology of HKUST-1. The collapse of the HKUST-1 structure is ascribed to water competing with organic ligand or CDs to coordinate with Cu^{2+} in HKUST-1, resulting in the collapse of the CDs@HKUST-1 structure with the release of CDs. The FT-IR spectrum of CDs@HKUST-1 after treating with water was also recorded, as shown in Fig. S10.‡ It was found that the characteristic peaks of CDs, including C–H stretching (2983 and 2900 cm^{-1}), C–O

© 2023 The Author(s). Published by the Royal Society of Chemistry

stretching (1076 cm^{-1}), and C–N (1024 cm^{-1}) disappeared. This highlights that CDs were released from the composite. Moreover, atomic absorption spectroscopy was performed to investigate the release of Cu^{2+} content from the composite after the addition of water. The Cu^{2+} content in the supernatant was found to be 111.90 ppm, confirming that the Cu^{2+} was released after the collapse of the HKUST-1 structure. Due to the strong affinity of Cu^{2+} toward water, water molecules could interact with Cu^{2+} by replacing the ligand and CDs. This can induce the dissociation of CDs@HKUST-1 as well as the exclusion of the fluorescence quencher (Cu^{2+}) and fluorescent CDs. Consequently, the electron transfer from CDs to an unoccupied Cu 3d orbital was subsequently blocked, leading to the recovery of the fluorescence of CDs.

4 Conclusions

In summary, CDs@HKUST-1 was successfully designed and synthesized, with the encapsulation of CDs into the MOF framework *via* a simple ultrasonic irradiation method. The prepared CDs@HKUST-1 was demonstrated, for the first time, as a turn-on fluorescent sensor for the detection of water in organic solvents *via* the inhibition of photo-induced electron transfer (PET). The CDs@HKUST-1 could detect water in ethanol, acetone, and acetonitrile with broad detection ranges and low LODs. The fluorogenic change during the sensing process could be observed by the naked eye under UV light (365 nm). The detection mechanism is related to the suppression of the PET process, driven by the dissociation of CDs@HKUST-1 in the presence of water. Additionally, by combining a smartphone with CDs@HKUST-1, a simple and portable sensing platform for on-site and real-time monitoring of water in organic solvents was successfully established. Consequently, the present work is a promising model for the design and fabrication of sensory materials for the detection of trace water in biofuel ethanol.

Conflicts of interest

There are no conflicts of interest to declare.

Acknowledgements

This work was financially supported by the Materials Chemistry Research Center (MCRC), Research and Graduate Studies, Khon Kaen University, Thailand.

References

1 H. S. Jung, P. Verwilst, W. Y. Kim and J. S. Kim, Fluorescent and colorimetric sensors for the detection of humidity or water content, *Chem. Soc. Rev.*, 2016, **45**, 1242–1256.

2 T. Wehner, K. Mandel, M. Schneider, G. Sextl and K. Müller-Buschbaum, Superparamagnetic luminescent MOF@Fe_3O_4/SiO_2 composite particles for signal augmentation by magnetic harvesting as potential water detectors, *ACS Appl. Mater. Interfaces*, 2016, **8**, 5445–5452.

3 Z. Zhang, T. Zhong and G. Wang, Zn-MOF74 as a "turn-on" fluorescent chemosensor for recognition and detection of water in acetone and Al^{3+} in ethanol with high selectivity and sensitivity, *J. Photochem. Photobiol., A*, 2022, **431**, 114052.

4 Y. Y. Liang, Automation of Karl Fischer water titration by flow injection sampling, *Anal. Chem.*, 1990, **62**, 2504–2506.

5 L. E. Harris, W. L. Budde and J. W. Eichelberger, Direct analysis of water samples for organic pollutants with gas chromatography-mass spectrometry, *Anal. Chem.*, 1974, **46**, 1912–1917.

6 R. Gruden, A. Buchholz and O. Kanoun, Electrochemical analysis of water and suds by impedance spectroscopy and cyclic voltammetry, *J. Sens. Sens. Syst.*, 2014, **3**, 133–140.

7 J. van den Broeke and T. Koster, *ICT for Smart Water Systems: Measurements and Data Science, The Handbook of Environmental Chemistry*, Springer, Cham, 2021, vol. 102, pp. 283–314.

8 N. Kong, H. Yuan, H. Zhou, Y. Zhao and S. Zhang, Colorimetric detection of water content in organic solvents *via* a smartphone with fluorescent Ag nanoclusters, *Anal. Methods*, 2021, **13**, 2722–2727.

9 Y. Wu, J. Ji, Y. Zhou, Z. Chen, S. Liu and J. Zhao, Ratiometric and colorimetric sensors for highly sensitive detection of water in organic solvents based on hydroxyl-containing polyimide-fluoride complexes, *Anal. Chim. Acta*, 2020, **1108**, 37–45.

10 Y. Zhan, F. Luo, L. Guo, B. Qiu, Y. Lin, J. Li, G. Chen and Z. Lin, Preparation of an efficient ratiometric fluorescent nanoprobe (m-CDs@$[Ru(bpy)_3]^{2+}$) for visual and specific detection of hypochlorite on site and in living cells, *ACS Sens.*, 2017, **2**, 1684–1691.

11 Q. Yao, S. Lu, F. Lin, T. Zhao, L. Zhao and X. Chen, A co-precipitation strategy for making a ratiometric pH nanosensor for intracellular imaging, *Sens. Actuators, B*, 2017, **250**, 484–490.

12 Q. Zhang, J. Wang, A. M. Kirillov, W. Dou, C. Xu, C. Xu, L. Yang, R. Fang and W. Liu, Multifunctional Ln–MOF luminescent probe for efficient sensing of Fe^{3+}, Ce^{3+}, and acetone, *ACS Appl. Mater. Interfaces*, 2018, **10**, 23976–23986.

13 G. Qin, Y. Kong, T. Gan and Y. Ni, Ultrathin 2D Eu^{3+}@Zn-MOF nanosheets: A functional nanoplatform for highly selective, sensitive, and visualized detection of organochlorine pesticides in a water environment, *Inorg. Chem.*, 2022, **61**, 8966–8975.

14 J. Ye, R. F. Bogale, Y. Shi, Y. Chen, X. Liu, S. Zhang, Y. Yang, J. Zhao and G. Ning, A water-stable dual-channel luminescence sensor for UO_2^{2+} ions based on an anionic terbium(III) metal–organic framework, *Chem.–Eur. J.*, 2017, **23**, 7657–7662.

15 L. Liu, Q. Chen, J. Lv, Y. Li, K. Wang and J.-R. Li, Stable metal-organic frameworks for fluorescent detection of tetracycline antibiotics, *Inorg. Chem.*, 2022, **61**, 8015–8021.

16 X. Zhou, J. Dong, Y. Zhu, L. Liu, Y. Jiao, H. Li, Y. Han, K. Davey, Q. Xu, Y. Zheng and S.-Z. Qiao, Molecularscalpel to chemically cleave metal–organic frameworks for induced phase transition, *J. Am. Chem. Soc.*, 2021, **143**, 6681–6690.

© 2023 The Author(s). Published by the Royal Society of Chemistry

17 L. Song, Y.-W. Wu, W.-X. Chai, Y.-S. Tao, C. Jiang and Q.-H. Wang, Fluorescence quenching of a europium coordination compound for the detection of trace amounts of water: uncovering the response mechanism by structural confirmation, *Eur. J. Inorg. Chem.*, 2015, 2264–2271.

18 J.-X. Wu and B. Yan, A dual-emission probe to detect moisture and water in organic solvents based on green-Tb^{3+} post-coordinated metal–organic frameworks with red carbon dots, *Dalton Trans.*, 2017, **46**, 7098–7105.

19 F. Cheng, R. Fu, Y. Wen, Y.-Y. Yang, C. Zeng, Y. Zhang, S. Hu and X. Wu, A new Cd based metal–organic framework for quick and convenient detection of trace water in isopropanol and 1,4-dioxane, *J. Mater. Chem. C*, 2018, **6**, 12341–12346.

20 B. Li, W. Wang, Z. Hong, E.-S. M. El-Sayed and D. Yuan, Ratiometric fluorescence detection of trace water in an organic solvent based on bimetallic lanthanide metal–organic frameworks, *Chem. Commun.*, 2019, **55**, 6926–6929.

21 J.-P. Gao, R.-X. Yao, X.-H. Chen, H.-H. Li, C. Zhang, F.-Q. Zhang and X.-M. Zhang, Blue luminescent N,S-doped carbon dots encapsulated in red emissive Eu-MOF to form dually emissive composite for reversible anti-counterfeit ink, *Dalton Trans.*, 2021, **50**, 1690–1696.

22 Y. Yu, G. Huang, X. Luo, W. Lin, Y. Han, J. Huang and Z. Li, Carbon dots@Cu metal–organic frameworks hybrids for ratiometric fluorescent determination of pesticide thiophanate-methyl, *Microchim. Acta*, 2022, **189**, 325.

23 L. Yu, Q. Zheng, H. Wang, C. Liu, X. Huang and Y. Xiao, Double-color lanthanide metal–organic framework based logic device and visual ratiometric fluorescence water microsensor for solid pharmaceuticals, *Anal. Chem.*, 2020, **92**, 1402–1408.

24 X.-M. Tian, S.-L. Yao, C.-Q. Qiu, T.-F. Zheng, Y.-Q. Chen, H. Huang, J.-L. Chen, S.-J. Liu and H.-R. Wen, Turn-On luminescent sensor toward Fe^{3+}, Cr^{3+}, and Al^{3+} based on a Co(II) metal–organic framework with open functional sites, *Inorg. Chem.*, 2020, **59**, 2803–2810.

25 Y. Qin, Y. Bai, P. Huang and F.-Y. Wu, Dual-emission carbon dots for ratiometric fluorescent water sensing, relative humidity sensing, and anticounterfeiting applications, *ACS Appl. Nano Mater.*, 2021, **4**, 10674–10681.

26 J. Yang, Z. Li and Q. Jia, Design of dual-emission fluorescence sensor based on Cu nanoclusters with solvent-dependent effects: Visual detection of water *via* a smartphone, *Sens. Actuators, B*, 2019, **297**, 126807.

27 M. Li, T. Chen, J. J. Gooding and J. Liu, Review of carbon and graphene quantum dots for sensing, *ACS Sens.*, 2019, **4**, 1732–1748.

28 A. Abbas, T. A. Tabish, S. J. Bull, T. M. Lim and A. N. Phan, High yield synthesis of graphene quantum dots from biomass waste as a highly selective probe for Fe^{3+} sensing, *Sci. Rep.*, 2020, **10**, 21262.

29 J. Tang, X. Ma, J. Yang, D.-D. Feng and X.-Q. Wang, Recent advances in metal–organic frameworks for pesticide detection and adsorption, *Dalton Trans.*, 2020, **49**, 14361–14372.

30 X. Yan, H. Qu, Y. Chang, W. Pang, Y. Wang and X. Duan, Surface engineering of metal–organic framework prepared on film bulk acoustic resonator for vapor detection, *ACS Appl. Mater. Interfaces*, 2020, **12**, 10009–10017.

31 L. Jin, C. Liu, N. An, Q. Zhang, J. Wang, L. Zhao and Y. Lu, Fluorescence turn-on detection of Fe^{3+} in pure water based on a cationic poly(perylenediimide) derivative, *RSC Adv.*, 2016, **6**, 58394–58400.

32 X. Fu, R. Lv, J. Su, H. Li, B. Yang, W. Gu and X. Liu, A dual-emission nano-rod MOF equipped with carbon dots for visual detection of doxycycline and sensitive sensing of MnO4, *RSC Adv.*, 2018, **8**, 4766–4772.

33 O. Xu, S. Wan, J. Yang, H. Song, L. Dong, J. Xia and X. Zhu, Ni-MOF functionalized carbon dots with fluorescence and adsorption performance for rapid detection of Fe (III) and ascorbic acid, *J. Fluoresc.*, 2022, **32**, 1743–1754.

34 S. K. Sharma, M. Micic, S. Li, B. Hoar, S. Paudyal, E. M. Zahran and R. M. Leblanc, Conjugation of carbon dots with β-Galactosidase enzyme: surface chemistry and use in biosensing, *Molecules*, 2019, **24**, 3275.

35 H. Li, W. Han, R. Lv, A. Zhai, X.-L. Li, W. Gu and X. Liu, Dual-function mixed-lanthanide metal–organic framework for ratiometric water detection in bioethanol and temperature sensing, *Anal. Chem.*, 2019, **91**, 2148–2154.

© 2023 The Author(s). Published by the Royal Society of Chemistry